

Barkhausen-like steps and magnetic frustration in doped $\text{La}_{0.67-x}\text{A}_x\text{Ca}_{0.33}\text{MnO}_3$ ($A = \text{Ce}, \text{Y}$)G. Alejandro,¹ L. B. Steren,^{1,*} A. Caneiro,¹ J. Cartes,² E. E. Vogel,² and P. Vargas³¹*Centro Atómico Bariloche and Instituto Balseiro, CNEA-UNC, (8400) San Carlos de Bariloche, Argentina*²*Department of Physics, Universidad de La Frontera, Temuco, Chile*³*Department of Physics, Universidad Técnica Federico Santa María, Valparaíso, Chile*

(Received 16 July 2005; revised manuscript received 14 October 2005; published 17 February 2006)

We present dc magnetization experiments performed on the doped, polycrystalline system $\text{La}_{0.67-x}\text{A}_x\text{Ca}_{0.33}\text{MnO}_3$ ($A = \text{Ce}, \text{Y}$). The ceramic samples have been obtained by the nitrate decomposition route and structurally characterized by powder x-ray diffraction. Hysteresis loops reveal an exciting and nonrepetitive multistep structure of Barkhausen-like jumps in the low fields region, up to 50 Oe. We discuss our results in terms of a collective response of magnetic moments pinned by frustration due to the competition among different exchange interactions present in the compounds. A simple Ising Hamiltonian with in-plane ferromagnetic interactions and randomly mixed off-plane interactions is introduced to model this hypothesis. Computer simulations based on this model allow us to reproduce most of the features observed in the hysteresis curves, allowing a qualitative understanding of the complex magnetic behavior of this family of manganites.

DOI: 10.1103/PhysRevB.73.054427

PACS number(s): 75.60.Ej, 75.50.Lk, 75.10.-b

I. INTRODUCTION

In a previous work,¹ Alejandro *et al.* presented a systematic investigation of the magnetic and transport properties of the cerium-doped compound $\text{La}_{0.47}\text{Ce}_{0.2}\text{Ca}_{0.33}\text{MnO}_3$. The study reveals that there is a strong correlation between these properties. A comparative analysis of those results suggests that a magnetically frustrated state develops at low temperatures ($T \leq 70$ K). The first experimental evidence of magnetic frustration found in this compound was the incomplete saturation of the magnetic moments at low temperatures and high fields. Another signature of this behavior was observed in the zero-field-cooled (ZFC) and field-cooled (FC) magnetization vs temperature curves. A maximum in the ZFC curve and a noticeable plateau in all the FC curves below the maximum temperature, T_F , independently of the cooling field, suggest a freezing of the spin system. Further indication for the setting up of a glassy state was found in the S shape of the M vs H virgin curves below T_F . This S behavior has been previously observed in a wide variety of spin-glasses below the freezing temperature² and therefore reinforces the hypothesis of the existence of a frustrated, glassy state in $\text{La}_{0.47}\text{Ce}_{0.2}\text{Ca}_{0.33}\text{MnO}_3$. Some peculiar features of the resistivity and magnetoresistance reported in Ref. 1 add more evidence for the magnetic frustration of the system. The results were analyzed in terms of short-range ordered regions that are probably embedded in a frustrated matrix or coupled forming a cluster-glass system. This behavior is attributed to the intrinsic cation disorder and consequent structural distortions of these compounds. As occurs in $\text{La}_{0.67-x}\text{Y}_x\text{Ca}_{0.33}\text{MnO}_3$ compounds,³ magnetic frustration in cerium-doped manganites would arise from the competition of ferromagnetic (FM) double-exchange and antiferromagnetic (AFM) superexchange interactions in a background of structural disorder.

With the aim of shedding some light to the issue of magnetic frustration in these compounds, we have performed very detailed magnetization measurements in

$\text{La}_{0.67-x}\text{A}_x\text{Ca}_{0.33}\text{MnO}_3$ ($A = \text{Ce}, \text{Y}$) compounds. In Sec. II, we describe the sample preparation route and the measuring setup, whereas the experimental results are presented in Sec. III. In Sec. IV we introduce a simple theoretical model to qualitatively account for the most interesting features of the hysteresis curves, and finally we summarize our conclusions in Sec. V.

II. EXPERIMENTAL SETUP, SAMPLE PREPARATION, AND CHARACTERIZATION

Powder ceramic samples of $\text{La}_{0.67-x}\text{Ce}_x\text{Ca}_{0.33}\text{MnO}_3$ with $x = 0, 0.1, 0.2$ (labeled as C0, C10 and C20, respectively), and $\text{La}_{0.47}\text{Y}_{0.2}\text{Ca}_{0.33}\text{MnO}_3$ (labeled as Y20) were prepared using the nitrate decomposition route in the former cases and liquid mix in the last one. The final calcination treatments for the Ce-doped and Y-doped samples were done at 1450 °C and 1200 °C, respectively. The incorporation of cerium or yttrium cations in the perovskite lattice was monitored by x-ray diffraction measurements, concluding that our samples are essentially single phased. For our higher Ce-doped sample, a segregation of less than 0.6 wt. % cerium oxide was found, i.e., only a 3.6% of the cerium ions are out of the perovskite compound.¹

The chemical composition of the samples has been checked by EDX-SEM analysis. Magnetization measurements were performed alternatively in a superconducting quantum device (SQUID) and in a vibrating sample magnetometer (VSM) from $T = 5$ K to $T = 300$ K, and magnetic fields, H , up to 50 kOe.

III. EXPERIMENTAL RESULTS

Figure 1 shows the magnetic hysteresis (M - H) curve of the C20 sample. Similar curves were measured for the other Ce- and Y-doped samples. The saturation magnetization (M_{sat}) is lower than the theoretical value ($\approx 3.8 \mu_B$) expected for a full polarization of the Mn spin-system. Furthermore,

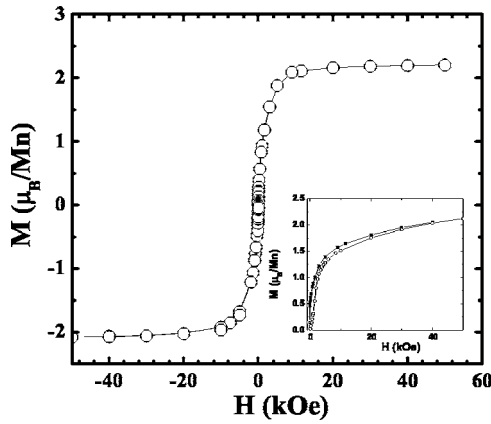


FIG. 1. Magnetization vs magnetic field curve of the $\text{La}_{0.47}\text{Ce}_{0.20}\text{Ca}_{0.33}\text{MnO}_3$ sample, measured at $T=5$ K. Inset: detail of the initial branch of the loop, including the virgin curve.

for the Ce-doped samples we observe that M_{sat} considerably decreases when the concentration of Ce ions increases, indicating that doping with cerium progressively frustrates the FM alignment of the Mn spins. The magnetization loops reveal a very high polarizability at low magnetic fields, exhibiting very small values of coercive field. Though these or similar features are not unusual in many manganites, distinctive and very curious characteristics arise in these doped compounds.

Figures 2(a)–2(c) show in detail the low field region of the hysteresis loops for the samples C20, Y20, and C0 samples. We can observe that the Ce- and Y-doped samples present similar features in their hysteresis curves. However, striking differences arise when comparing these results to those of ferromagnetic $\text{La}_{0.67}\text{Ca}_{0.33}\text{MnO}_3$ ($x=0$). While the hysteresis loop of the undoped (C0) sample [Fig. 2(c)] exhibits a completely smooth variation at this field scale, the Ce- and Y-doped compounds present a much more complex structure characterized by a pattern of discrete jumps of magnetization. These magnetization jumps occur in the region of low magnetic fields, never larger than 50 Oe. Moreover, the magnitude of these jumps is about $0.1 \mu_B$ per formula unit. The very last features resemble the phenomenon usually known as “Barkhausen jumps,” an effect that has been very much studied in Fe alloys and whose origin was attributed to domain-wall motion.⁴

In order to analyze the influence of progressive doping on the stepped structure of the M - H loops, we compare the results obtained on the cerium-doped samples (Fig. 3). A careful observation of the curves of both samples reveals that the magnetization jumps of the C20 sample are more defined and abrupt, while these signatures are smoother in the C10 one. The overall magnetization variation is about $1 \mu_B/\text{Mn}$ for the $x=0.2$ sample, decreasing to about $0.8 \mu_B/\text{Mn}$ for the $x=0.1$ sample. The jumps are therefore associated with the extra doping and consequent distortion of the $\text{La}_{0.67}\text{Ca}_{0.33}\text{MnO}_3$ parent compound. The other interesting feature observed in the C20 loops is that they present three jumps in most of the runs. The fact that no more than three of these jumps are observed is important for the theoretical model introduced below.

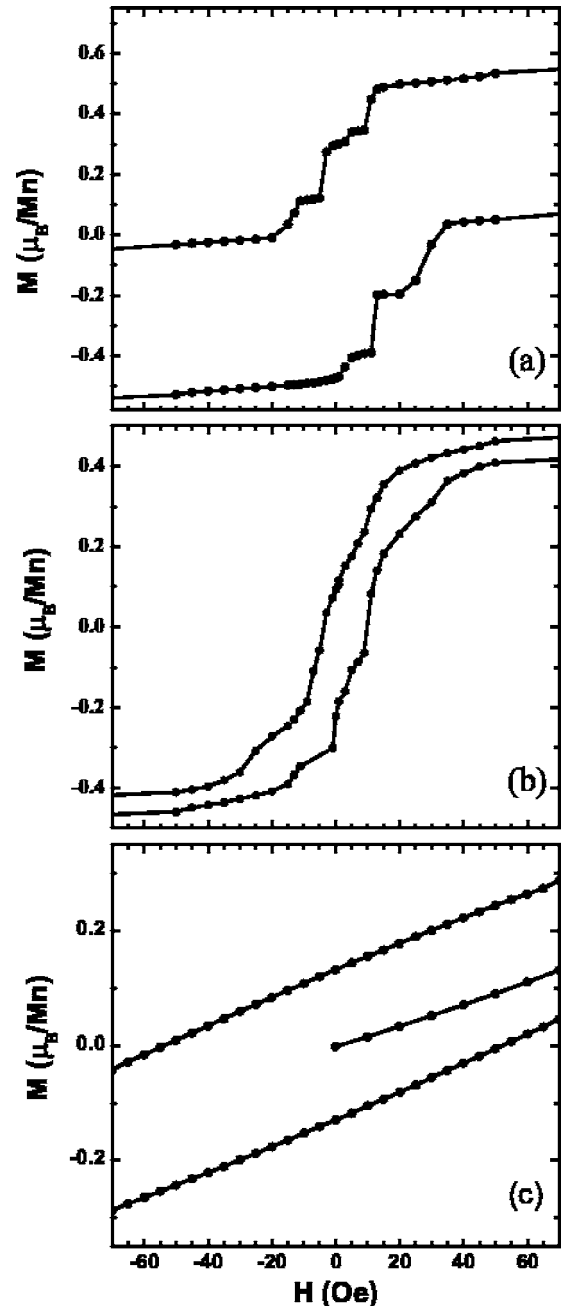


FIG. 2. Detail of the low-field region of the hysteresis loops of the (a) C20, (b) Y20 and (c) C0 samples, measured at 5 K.

Another characteristic of the jumps can be appreciated from Fig. 3(a). In this figure, two consecutive runs of the C20 loops are presented. A magnetic field of 50 000 Oe has been first applied to the sample. Then, the field has been swept between ± 4000 Oe. The last field is high enough to close the irreversible zone of the successive magnetization loops. As we are mainly concerned with the low field region, we have plotted the results falling in the $-50 \text{ Oe} \leq H \leq 50 \text{ Oe}$ range. The curves put in evidence the nonrepetitive character of the jumps. A similar behavior has been recently reported for mixed-phase manganites.⁵ The referred results, however, were observed at much higher fields and only in the virgin leg of the loop. The magnetization jumps measured in

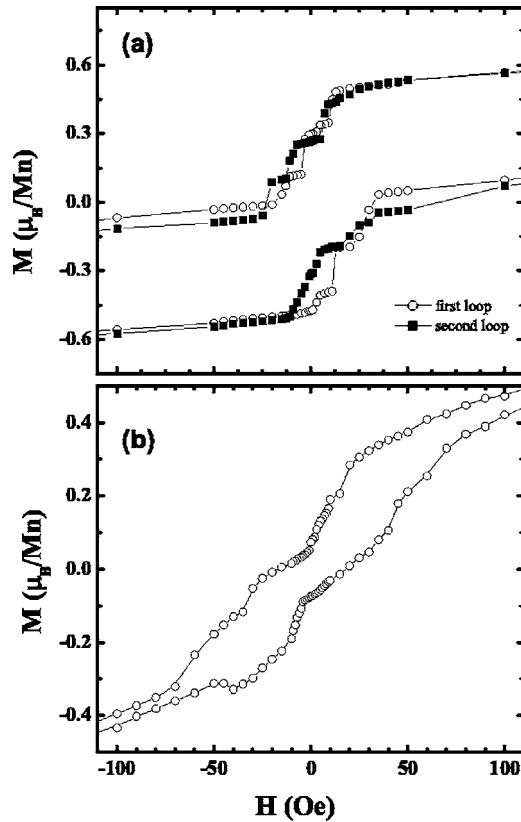


FIG. 3. M - H low-field region for the (a) C20 and (b) C10 samples, measured at 5 K. Two different measurements have been plotted for the C20.

our samples are not only of small size and randomly situated in the field scale as the measure is repeated. They are also activated in both increasing and decreasing branches of the loops, even after having submitted the system to fields larger than the saturation field.

We have also investigated the temperature dependence of the magnetization jumps. Figure 4 shows magnetization loops of the C20 sample, measured at $T=35$ K and $T=70$ K. It is evident from the comparison of Figs. 3 and 4 that the jump structure is considerably blurred as the temperature is increased. Moreover, the nonrepetitive character of the magnetization process at low fields is progressively lost with increasing temperature, i.e., at the higher temperature [Fig. 4(b)], the two consecutive measurements are almost coincident. Finally, it can be seen that the loop measured at 70 K is bottle-necked, and is particularly strangled at low field.

Further information about the thermal activation of the magnetization jumps can be obtained from the ZFC-FC magnetization vs temperature curves⁶ shown in Fig. 5. In the low temperature regime ($T_F < 70$ K), the ZFC curve tends to zero magnetization while the FC curve remains nearly constant. The ZFC curve passes through a maximum around T_F and both curves merge into a single one above 160 K. We remark that the step structure of the M - H curves appears below $T \approx T_F$. Moreover, there is a direct correlation between the magnitude of the irreversibility in the ZFC-FC vs T curves and the “sharpness” of the step structure. Both aspects sug-

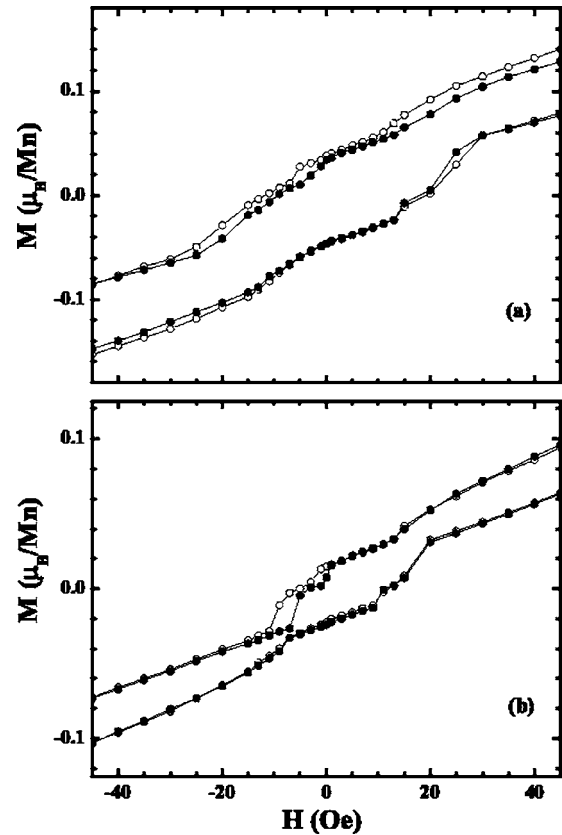


FIG. 4. M - H low-field region for the C20 sample, measured at (a) $T=35$ K and (b) $T=70$ K.

gest that the magnetization jumps are directly associated with the low temperature magnetic frustrated phase of the compound. The other samples present a similar behavior.

IV. DISCUSSION

To explain qualitatively our experimental results we propose a simple model based on an Ising Hamiltonian. In the next paragraph we summarize the main signatures of the magnetization loops of our samples, before introducing the theoretical model. The $\text{La}_{0.67-x}\text{A}_x\text{Ca}_{0.33}\text{MnO}_3$ ($x=0$) com-

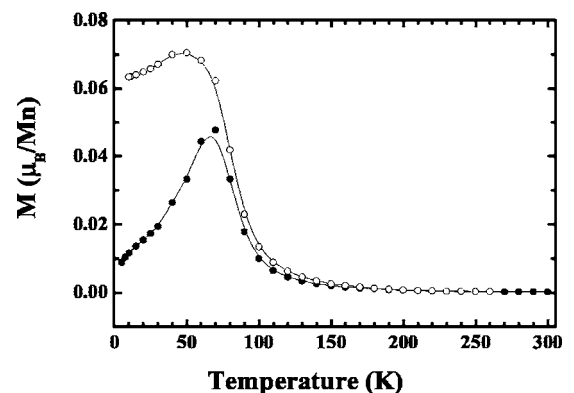


FIG. 5. ZFC (●) and FC (○) magnetization curves for the C20 sample measured with $H=50$ Oe.

pound presents a hysteresis curve of a typical ferromagnet with the virgin curve inside the loop. As the A-dopant content increases, this behavior changes and particular features are noticed. First, at low fields, $H = \pm 50$ Oe, the magnetization changes in discrete steps, which can be viewed as avalanches of spins similar to Barkhausen jumps. Typically, our magnetization loops exhibit three sharp steps. The magnitude of the magnetization jumps, not being the same for all the jumps, has an average of $0.1 \mu_B/\text{Mn}$. Second, the loops are not repetitive: the magnetization steps occur at similar, but not exactly the same, values of the external magnetic field when data coming from different runs are compared. Third, the magnetization virgin curve falls outside the loops (see inset of Fig. 1). Finally, as the temperature increases, rounding effects in the steplike structure are observed: the magnitude of the jumps decreases and the loops become narrower. The previous features become weaker as the Ce or Y concentration is decreased, i.e., when the structure distortion decreases.⁷

We recall here that patterns of discrete and very sharp jumps in the magnetization curves of some manganites have been previously reported by several groups during the last years.^{5,8-14} Ceramic samples,⁸⁻¹¹ single crystals,^{12,13} and manganite films¹⁴ have revealed the presence of magnetization jumps. Many of them present frustrated characters like the mixed-phased manganites. Most of the cited papers reported the existence of very few and rather large magnetization jumps ($1 \mu_B/\text{Mn}$ or more), observed at $H \approx 15\,000$ Oe and very low temperatures. These jumps are only observed in the increasing-field branch of the magnetization loops, suggesting that after reaching saturation the samples have undergone some irreversible, field-induced transformation comparable to a martensitic transition in metallic alloys.^{5,9} More recently, Hardy *et al.*⁵ showed through detailed magnetization measurement the presence of smaller and multiple magnetization steps superimposed on the larger magnetization jumps in mixed-phase manganites. As stated before, these results were observed at $T < 2$ K and $H > 10\,000$ Oe, in the increasing-field branch of the magnetization loop and within the larger step of magnetization. The “return” branch of the loops appears completely smooth and absent of jumps. The smaller jumps tend to vanish above 1.75 K, though the larger steps persist even up to 5 K.

The steplike magnetization patterns reported in our work have several distinctive features. In spite of the fact that the magnetization jumps measured in our samples are of similar sizes, they appear in a different field range. Furthermore they are seen in both the increasing and decreasing field legs of the loops, indicating that this low field steplike behavior persists even after the sample’s magnetization is saturated. The small-jump patterns are not exactly reproducible, meaning that the position of the jumps varies slightly from measurement to measurement. The temperature dependence of our step structure is also different from the previous reported data, as no large magnetization jumps have been observed at any of the explored temperatures. The magnetic behavior of our samples suggests the setting up of a frustrated phase below a critical temperature, T_F . Below T_F , the steplike structure in the low magnetic field range appears in a quasi-symmetric pattern around zero field. These jumps are blurred

and of smaller size as the temperature is increased. The existence of significant differences between our results and the previous ones suggests that they probably have a different physical origin, presumptively associated with the kind of magnetic frustration involved.

Samples with narrow hysteresis curves suggest weak coupling or low values of the local fields due to competing interactions. This fact would allow a theoretical description based on mixed magnetic interactions. Let us further justify this proposal by considering first the case of LaMnO_3 , where antiferromagnetism (AFM) type A is present,^{15,16} namely, neighboring ferromagnetic (FM) planes alternate their orientation. It is possible to distinguish between in-plane (xy) FM interactions and off-plane (z axis) AFM interactions. As the La is substituted for Ca, Mn^{3+} changes to Mn^{4+} to compensate for the missing electron formerly coming from the La ions. This charge distribution favors FM double-exchange interactions, weakening the condition for AFM interactions, and therefore $\text{La}_{0.67}\text{Ca}_{0.33}\text{MnO}_3$ is ferromagnetic.

It is possible to think that lattice distortions induced by the doping of $\text{La}_{0.67-x}\text{A}_x\text{Ca}_{0.33}\text{MnO}_3$ with A cations (A = Ce, Y) indeed favors the formation of antiferromagnetic bonds along the z axis. That is to say that at low temperature and low magnetic fields antiferromagnetism could prevail in some sectors or clusters of the sample. Such bond configuration is randomly distributed across the sample and the A cations would play the role of pinning sectors with AFM interactions, as will be described below. This phenomenon should increase with A concentration, as found in the experiments.

We propose a plausible explanation for this phenomenon based on a collective response of spin-planes subject to anisotropic random local fields due to competition of nearest neighbor interactions of mixed character. We depart from usual random field or random bond models,^{17,18} guiding the distribution of bonds so anisotropic noise is superposed to an antiferromagnetic type-A phase. This procedure is reasonable because there are nonisotropic interactions between Mn pairs, whose magnitude depends on the neighboring atoms (La, A, or Ca) and on the angles and distances involved in the Mn-O-Mn links. A complete Hamiltonian describing this system would be extremely complex and almost impossible to deal with. For this reason, we have retained the most significant features of this model bearing in mind the original antiferromagnetism of type A of the stoichiometric sample. Our main assumptions are the following: the magnetic interactions in the xy plane are assumed to be FM and all of the same strength; part of the interactions along the z axis are AFM while the rest are FM; the strength of these interactions depends on the surrounding ions and will be varied in the simulations below. We will show that these competing interactions would lead to magnetic frustration and the formation of cluster-glass sectors in the system.

According to these hypotheses, a large number of magnetic atoms will respond ferromagnetically, except where the local abundance of AFM interactions will define sectors where partial AFM type-A ordering is possible. These sectors will respond to the external field as a whole since the weakest linked Mn atom would flip immediately, weakening the local field condition on the neighboring magnetic ions, and

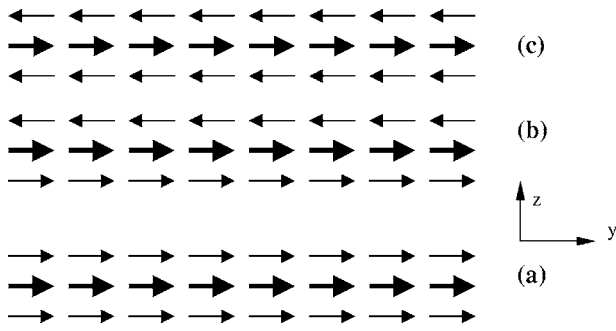


FIG. 6. Three possible magnetic fields situations that produce magnetization avalanches. In all cases the in-plane ferromagnetic interactions are satisfied, while the off-plane antiferromagnetic interactions (z direction) are represented in three different conditions. From bottom to top: (a) a positive external magnetic field is needed to prevent the central plane from overturning completely; (b) the central plane is free (subject to zero field from its neighboring planes); (c) the interactions of the central plane are satisfied and a negative external magnetic field is needed to overturn the central plane.

thus causing a small avalanche. This situation occurs independently in different clusters through the material where such a local field condition is achieved. After the overturn of a planar sector, the planes that lay above and below it will follow this process once the external field tunes to the new local field condition.

Following this model three critical fields are possible for such avalanches in accordance with the discussion of Fig. 3 above. Such critical fields are illustrated in Fig. 6. For simplicity we assume that all the interactions along the z axis are antiferromagnetic and that the magnetic field is applied in the y direction. In the scheme (a), a forced ferromagnetic ordering is possible by means of an external magnetic field along the positive y direction; when this field is decreased below a critical value H_+ one of the planes (the central one in this figure, for instance) will overturn. In (b) the central plane is free and so a critical field H_0 close to zero will be enough to overturn the central reference plane. In (c) the interactions on the central plane are satisfied and a negative external magnetic field (pointing to the y direction) of magnitude larger than $|H_-|$ is needed to overturn the central reference plane in order to achieve ferromagnetic orientation in the negative y direction.

This picture can produce up to three possible values of magnetic field for magnetization jumps to occur. However, the previous picture is an oversimplification of the reality in which several different local fields occur within a plane. Thus, the weakest pinned magnetic moment in a plane can trigger the overturning mechanism. The order in which these local “domains” overturn is not always the same, explaining why no return-point memory is observed. The magnitude of the magnetization avalanches depends on the order in which these AFM sectors overturn due to local frustrations. Smaller jumps could also occur, when only a fraction of a plane overturns and the rest remains pinned due to variations in the local fields. These frustration effects are also responsible for the virgin curve having less magnetization than the lower hysteresis branch.

The magnetization reversal mechanism described above will only take place in small sectors of the sample where the concentration of A atoms allows this ordering to some extent. The volume occupied by AFM clusters will increase with the dopant concentration in such a way that the overall turnover of magnetic moments will account for approximately $1 \mu_B$ for the case of $x=0.2$. The rest of the sample remains essentially ferromagnetic, which agrees well with the behavior shown in Fig. 1.

Although the picture described above corresponds to a collective response of the system, it is possible to attempt a qualitative and simple simulation of the main features of the central region of the hysteresis curves. We propose an Ising Hamiltonian approach that applies locally to those sectors of the sample where dopant atoms tend to cluster. Such a component of the total Hamiltonian can be written as

$$\mathcal{H} = \sum_{i < j} K_{ij} S_i S_j - \sum_i H S_i, \quad (1)$$

where K_{ij} represents the exchange interaction between manganese ions at sites i and j respectively, the sum is restricted to nearest neighbors only, and H is the external magnetic field. To simulate the competing interactions depicted previously, we will consider that all in-plane exchange interactions are FM and of the same strength: $K_{ij} = -J$ for the xy plane; the off-plane (z axis) interactions can be AFM, $K_{ij} = +\alpha J$ in concentration ζ ($0 < \zeta < 1$), or FM $K_{ij} = -\alpha J$ in concentration $1 - \zeta$. Both α and J are positive real numbers. The occupation of these positive and negative interactions is random. These two interactions are assumed to have the same strength in order to assign to only two parameters (ζ and α) all the variations of this qualitative model.

Such a Hamiltonian will construct sectors of the sample, designated as clusters from now on, where ordering in the xy planes will tend to be ferromagnetic, while interactions along the z axis will tend to antiferromagnetically order some regions of a few consecutive planes. Several clusters of the same size were prepared independently and in a random way, and the parameters ζ and α were varied extensively within each cluster. A Monte Carlo process was used to examine the evolution of the system in the configuration space, and the Metropolis algorithm was invoked to introduce temperature effects by using Boltzmann’s statistics. The magnetic field H is increased in steps equivalent to one spin-flip. The external magnetic field H and the temperature are introduced in the model in units of J .

The virgin magnetization curves have been simulated starting the calculations at $H=0$. Two complete curves have been calculated in all the cases so as to examine the reversibility of the magnetization process. Our simulations considered variations of cluster size from $6 \times 6 \times 6$ to $12 \times 12 \times 12$, but no significant changes have been observed in the calculated results. For this reason, most of the calculations have been performed on $6 \times 6 \times 6$ clusters, in order to minimize the computing calculation time. The calculated loops (Fig. 7) qualitatively reproduce most of the features observed in the experimental ones. Namely, that the magnetization changes in steps, three as the number of most pronounced steps, the nonexact reproducibility of the loops, and that the

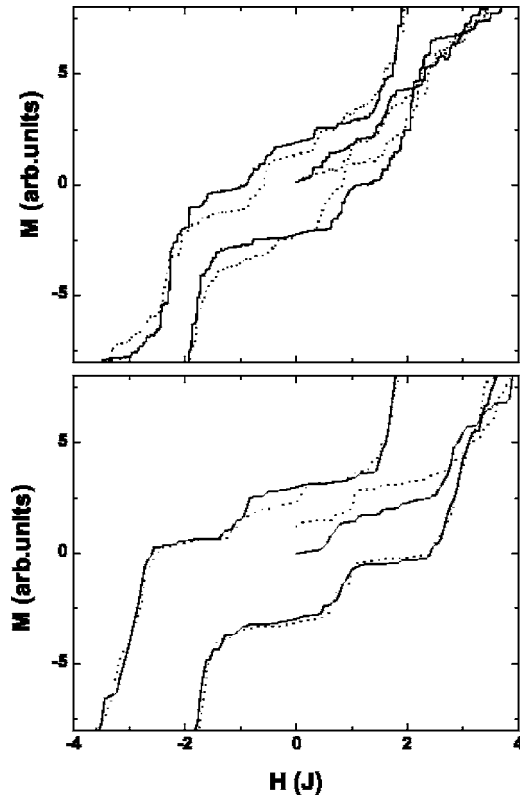


FIG. 7. Simulation of hysteresis loops for cluster sizes (bottom) $6 \times 6 \times 6$ and (top) $12 \times 12 \times 12$, using $J_z = \pm 2.0J$ (0.7%), $T = 0.3J$. Virgin curves and loops have been calculated for two different runs in each case.

virgin curves fall outside the main loops. The simulations shown in Fig. 7 uses the ζ and α values that better reproduces the measured loops characteristics (see comments below).

In Fig. 8 we present the dependence of the loops shape with the coupling strength, α . It can be seen that for small α values the jumps are sharp and short, while the virgin curve goes inside the loop. On the other hand, for large values of α the jumps are rounded, the magnetization process tends to be more repetitive, and the virgin curve goes inside the main loop. Similar results were obtained by varying ζ . The best set of parameters that leads to simulations closer to the measured curves is $\zeta = 0.7$ and $\alpha = 2$.

Studies on the statistics of the magnitude and position of the magnetization steps would be useful to further enlighten the mechanisms underlying the steplike behavior.

The temperature dependence of the loops was also examined using the best set of parameters on the $6 \times 6 \times 6$ cluster. In Fig. 9, calculated loops for different temperatures are shown. We observe that the loops narrow as the temperature is increased, while the step structure is somewhat preserved as it occurs in the experiments (see Fig. 4).

V. CONCLUDING REMARKS

The system $\text{La}_{0.67-x}\text{A}_x\text{Ca}_{0.33}\text{MnO}_3$ ($A = \text{Ce}, \text{Y}$; $x = 0.1, 0.2$) presents hysteresis loops with a steplike structure at low magnetic fields and low temperature. The shape of the loops is the same along different runs although consecutive cycles are not repetitive. The observed patterns of small magnetization jumps persist even after saturating the magnetic field, and furthermore, the virgin curves fall outside the main loop.

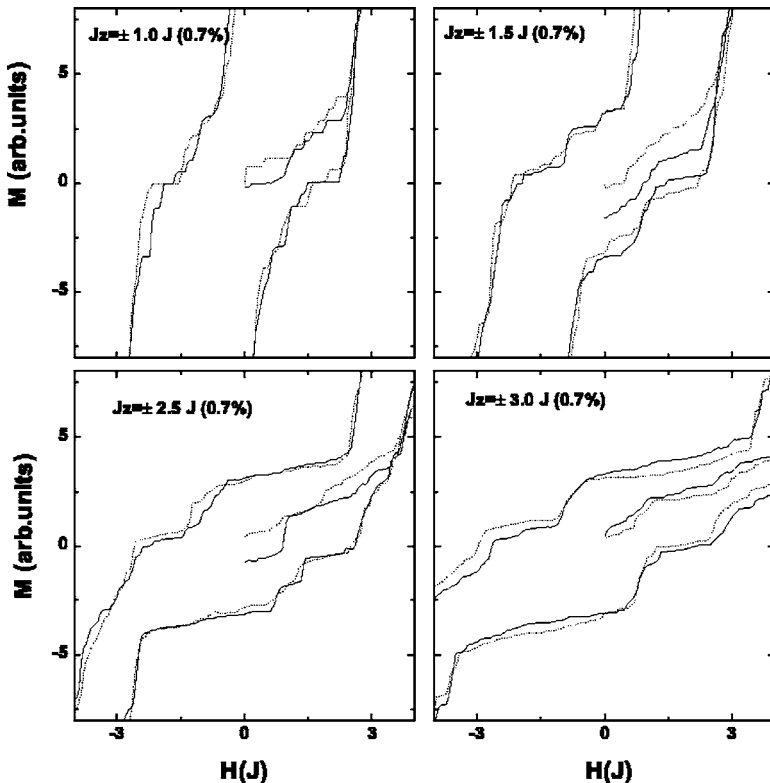


FIG. 8. Simulation of two consecutive hysteresis curves varying the strength of the interactions along the z axis, performed in an array $6 \times 6 \times 6$. The rest of the parameters are those of Fig. 6.

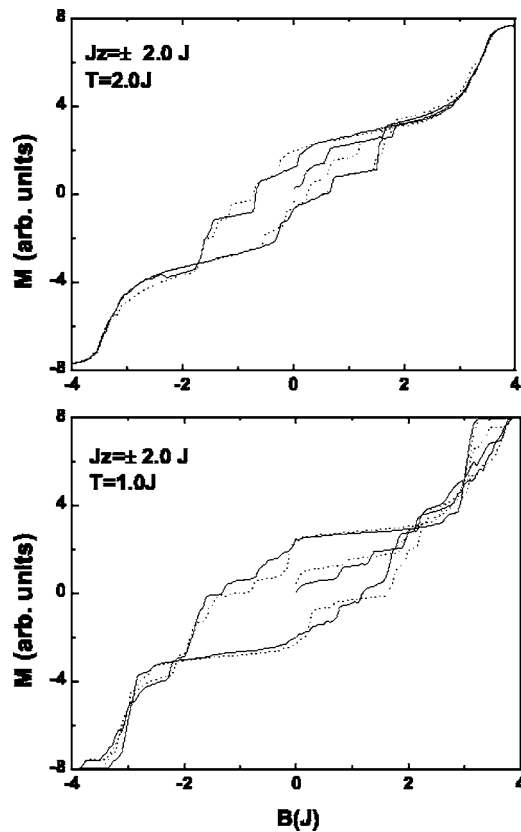


FIG. 9. Simulation of the temperature variation of the loops, using the same parameters of Fig. 6 in an array $6 \times 6 \times 6$.

These features reinforce the idea that the A -doping induces magnetic frustration into this system. Some sort of collective effect occurs in these systems, being capable of producing avalanches of magnetization once a single magnetic moment fluctuates, triggering a chain reaction or domino effect. We have noted that this phenomenon occurs in a variety of systems doped with different A cations and that it is more pronounced as the concentration of the A dopant is increased.

The experimental results were analyzed in terms of a model based on randomly mixed magnetic interactions. Our computer simulations using an Ising Hamiltonian lead to hysteresis loops resembling the experimental ones, explaining qualitatively the main features of the magnetization data. The picture used to describe our system consists of a soft ferromagnetic material with embedded clusters where mixed interactions, ferromagnetic and antiferromagnetic, are present and competing. Such clusters will respond to the external magnetic field depending of its strength. However, the randomness of the local fields inside the sample allows that different magnetic moments can trigger the flipping process, thus making each hysteresis loop essentially independent from the previous one. The observed magnetization jumps are then produced by the flipping of planes (or large regions of planes) within these partly antiferromagnetic clusters embedded in a soft ferromagnetic matrix.

ACKNOWLEDGMENTS

The authors are grateful for partial financial support from Fundación Antorchas, FONCyT 03-13297, CONICET, Millennium Scientific Nucleus “Condensed Matter Physics” P-02-054-F and Fondecyt Projects No. 1020993 and No. 1040354.

*Corresponding author. E-mail address: steren@cab.cnea.gov.ar

¹G. Alejandro, D. G. Lamas, L. B. Steren, J. E. Gayone, G. Zampieri, A. Caneiro, M. T. Causa, and M. Tovar, Phys. Rev. B **67**, 064424 (2003).

²K. Binder and A. P. Young, Rev. Mod. Phys. **58**, No. 4, 801 (1986), and references therein.

³G. Alejandro, M. T. Causa, M. Tovar, J. Fontcuberta, and X. Obradors, J. Appl. Phys. **87**, 5603 (2000).

⁴S. Zapperi, P. Cizeau, G. Durin, and H. E. Stanley, Phys. Rev. B **58**, 6353 (1998).

⁵V. Hardy, S. Majumdar, M. R. Lees, D. M. Paul, C. Yaicle, and M. Hervieu, Phys. Rev. B **70**, 104423 (2004).

⁶These curves were measured with an applied magnetic field of 50 Oe, larger than the coercive field of the sample.

⁷D. Lamas (private communication).

⁸R. Mahendiran, A. Maignan, S. Hébert, C. Martin, M. Hervieu, B. Raveau, J. F. Mitchell, and P. Schiffer, Phys. Rev. Lett. **89**, 286602 (2002).

⁹V. Hardy, A. Maignan, S. Hébert, C. Yaicle, C. Martin, M. Hervieu, M. R. Lees, G. Rowlands, D. M. Paul, and B. Raveau,

Phys. Rev. B **68**, 220402(R) (2003).

¹⁰L. M. Fisher, A. V. Kalinov, I. F. Voloshin, N. A. Babushkina, D. I. Khomskii, Y. Zhang, and T. T. M. Palstra, Phys. Rev. B **70**, 212411 (2004).

¹¹L. Ghivelder, R. S. Freitas, M. G. das Virgens, H. Martinho, L. Granja, G. Leyva, P. Levy, and F. Parisi, Phys. Rev. B **69**, 214414 (2004).

¹²F. M. Woodward, J. W. Lynn, M. B. Stone, R. Mahendiran, P. Schiffer, J. F. Mitchell, D. N. Argyriou, and L. C. Chapon, Phys. Rev. B **70**, 174433 (2004).

¹³Guixin Cao, Jincang Zhang, Shixun Cao, Chao Jing, and Xuechu Shen, Phys. Rev. B **71**, 174414 (2005).

¹⁴T. Wu and J. F. Mitchell, Phys. Rev. B **69**, 100405(R) (2004).

¹⁵B. C. Hauback, H. Fjellbag, and N. Sakai, J. Solid State Chem. **124**, 43 (1996).

¹⁶E. O. Wollan and W. C. Keohler, Phys. Rev. **100**, 545 (1955).

¹⁷O. Perković, K. Dahmen, and J. P. Sethna, Phys. Rev. Lett. **75**, 4528 (1995).

¹⁸K. Dahmen and J. P. Sethna, Phys. Rev. B **53**, 14872 (1996).